A NOVEL CLASS OF PLATELET ACTIVATING FACTOR ANTAGONISTS FROM *Phoma* sp.

MIN CHU, IMBI TRUUMEES, IJI GUNNARSSON, W. ROBERT BISHOP, WILLIAM KREUTNER, ANN C. HORAN, MAHESH G. PATEL, VINCENT P. GULLO and MOHINDAR S. PUAR

Schering-Plough-Research Institute,
2015 Galloping Hill Road, Kenilworth, NJ 07033, U.S.A.

(Received for publication October 19, 1992)

Four novel platelet activating factor (PAF) antagonists, Sch 47918, Sch 49026, Sch 49027 and Sch 49028, were isolated from the fermentation broth of the fungal culture, *Phoma* sp. (ATCC 74077). The structures of these compounds were elucidated by spectroscopic methods. The structure and stereochemistry of the first isolated component, Sch 47918, were confirmed by single crystal X-ray diffraction analysis. Sch 49028, the most active component, was found to inhibit PAF-induced human platelet aggregation *in vitro* with an IC_{50} of 1.26 μM. However, this compound was inactive *in vivo* at 5 mg/kg, iv against PAF-induced bronchospasm in guinea pigs.

Platelet activating factor (PAF, 1-*O*-alkyl-2-(*R*)-(acetylglyceryl)-3-phosphocholine) is a potential mediator of allergic[1,2] and non-allergic inflammatory[3] diseases. PAF binds to specific receptors on various cell types leading to diverse biological responses including platelet aggregation, leukocyte activation and hypotension.[4] The PAF receptor is a very attractive target for developing a new type of anti-allergic and anti-inflammatory drug. In recent years, the search for PAF antagonists has led to the discovery of a number of new natural products from microbial origin.[5~8] However, a majority of these compounds possesses the dialkylthiopiperazinedione moiety.[9] In the course of our screening program for novel PAF inhibitors, four macrocyclic compounds were discovered from the fermentation broth of a fungal culture. These compounds represent an uncommon 14-membered macrocyclic ring system with a bridged 6-membered ring. In this report, we describe the details of the identification and fermentation of the producting culture, the isolation, physico-chemical properties, structure elucidation and biological activities of the pure compounds.

Experimental

Taxonomy

Agar plugs, 2 × 2 mm, from 10 to 14-day old malt extract agar slants, incubated at 22°C, were used as the inoculum for morphological and cultural characteristics. Morphological characteristics were observed on plates of malt extract agar[10] incubated at 22°C for 10 to 12 days. Culture characteristics were observed on petri dishes containing malt extract, malt yeast, potato dextrose and CZAPEK's Dox agars[10] after 12 days at 22°C in the dark.

Fermentation

The initial stage inoculum for the fermentation of the PAF antagonists was prepared by transferring 2.5 ml of a frozen whole broth (at −20°C) to 50 ml of germination medium in 250 ml Erlenmeyer flasks. The germination medium (g/liter) consisted of Proteose peptone #3, 0.5%; sodium chloride, 0.5%; glucose, 2%; yeast extract, 0.3%; soy grits, 0.5%; and sodium potassium phosphate (monobasic) 0.5%. The pH

of the medium was adjusted to 7.0 prior to sterilization. The flasks were incubated at 30°C on a gyratory shaker at 300 rpm for 48 hours. For the second stage germination, a 2-liter Erlenmeyer flask containing 350 ml of the same medium was inoculated with 25 ml of the first stage germination and incubated as described above for 72 hours. Ten-liter fermentations were carried out in 14-liter fermentors (New Brunswick Scientific, Edison, N.J.) in a medium containing Neopeptone, 1%; and glucose, 4%. The pH of the medium was adjusted to 7.0 before sterilization. The second stage inoculum (3.5%) was used to initiate the fermentation which was conducted at 30°C with 4.5 liters/minute air flow and 400 rpm agitation for five days. An antifoam agent such as SAG (Union Carbide Corp., 50% solution) was added, if necessary, to the fermentors to control foam. During the course of the fermentation, production of the PAF-active complex in the whole broth was monitored using the PAF-induced platelet aggregation assay.

Isolation

The fermentation broth (20 liters) was extracted with ethyl acetate (80 liters) at harvest pH (see Scheme 1). The extract was evaporated *in vacuo* to a brown syrup. The syrup was dissolved in a minimum amount of dichloromethane - methanol (7 : 3) solvent mixture and loaded onto a Sephadex LH-20 column (700 ml). The column was eluted with the same solvent mixture. The early PAF active fractions which consisted mainly of Sch 47918, were combined based on TLC analysis (TLC conditions: silica gel plate, LK6DF Whatman; solvent, CH_2Cl_2 - MeOH 95 : 5; indicator, iodine chamber; Rf values of Sch 47918, Sch 49026, Sch 49027 and Sch 49028 are 0.71, 0.79, 0.44 and 0.41, respectively). The solvent volume was reduced until precipitation occurred. The pale yellow solid was readily precipitated by the addition of methanol, and then recrystallized with chloroform - methanol (3 : 7) to afford pure Sch 47918. The later fractions were

Scheme 1. Isolation of Sch 47918, Sch 49026, Sch 49027 and Sch 49028.

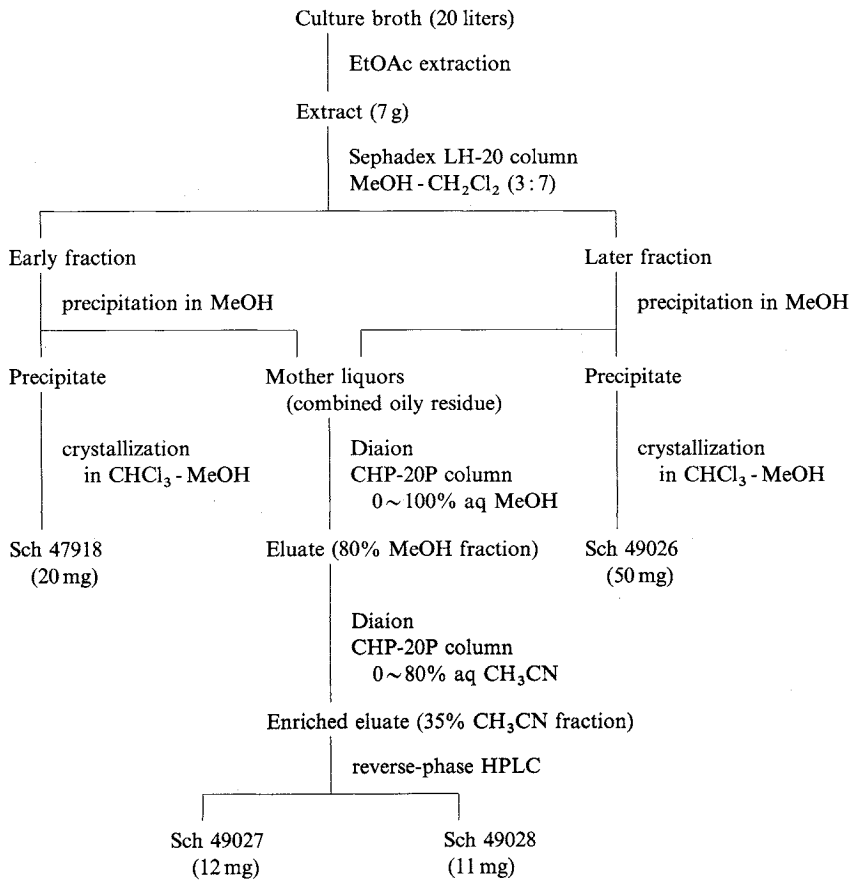

obtained as an active complex. Pure Sch 49026 was isolated from this complex by the same precipitation and recrystallization procedures used to obtain Sch 47918. The combined mother liquors from both precipitations were dried, and the residue was further purified by two consecutive Diaion CHP-20P gel columns (350 ml). The first was eluted with 0~100% aqueous MeOH gradient, and the second with 0~80% aqueous CH_3CN gradient. Final separation of Sch 49027 and Sch 49028 was achieved by reverse-phase HPLC under the following conditions: YMC-ODS 20 × 500 mm column, irregular 15 μm particles; mobile phase: 80% aqueous methanol; flow rate: 12 ml/minute; detection: UV at 210 nm, retention time; Rt = 23.6 and 33.8 minutes, respectively. This procedure yielded pure Sch 49027 and Sch 49028.

Spectroscopy

The melting points were measured on a MEL-TEMP apparatus (Laboratory Devices, Cambridge, MA) and are uncorrected. The optical rotations were measured on a Rudolph Research model 'AUTOPOL III' automatic polarimeter. IR spectra were obtained using a Nicolet FTIR model 10-MX instrument. UV spectra were recorded on a Hewlett Packard '8450 A' UV-vis spectrophotometer. CI and FAB-mass spectra were produced on a Hewlett Packard '5989 A' mass spectrometer using particle beam interface in methanol, and a Finnigan MAT-312 mass spectrometer in a glycerol-thioglycerol matrix, respectively. High resolution EI-MS were recorded on a Finnigan MAT-90 instrument using perfluoroalkene-225 (PFK) as a reference. Both ^1H and ^{13}C NMR spectra were obtained from Varian XL-300 instrument operating at 300 and 75 MHz, respectively.

In Vitro PAF Assay

Preparation of platelet-rich plasma (PRP): Human blood (50 ml) was collected from healthy donors. The blood (50 ml) was mixed with an anticoagulant solution (5 ml) containing sodium citrate (3.8%) and glucose (2%). Blood was centrifuged at 200 × g for 20 minutes and the supernatant PRP was carefully transferred into a polypropylene tube. Platelet-poor plasma (PPP) was prepared by centrifuging PRP at 800 × g for 15 minutes. PRP was used within 3 hours of drawing the blood.

Platelet aggregation assay: Platelet aggregation can be induced by addition of various platelet agonists, including PAF or thrombin, to PRP. Aggregation can be quantitated by measuring light transmission through PRP and comparing it to transmission through PPP. The aggregation assays were performed using a dual-channel aggregometer (Model 440, Chrono-Log Corp., Havertown, PA). PRP (0.45 ml) in aggregometer cuvettes was continually stirred (37°C). Solution of test compounds in DMSO or vehicle alone (final concentration of DMSO = 0.1%, v/v) were added to the PRP, followed by addition of PAF solutions to achieve a final concentration of $1 \sim 5 \times 10^{-8}$ M. Incubations were continued until the increase in light transmission reached a maximum (usually about 2 minutes). Values for inhibition were calculated by comparing maximal aggregation obtained in the absence and the presence of the compound. The IC_{50} was the concentration of compound at which 50% inhibition of aggregation occurred.

In Vivo PAF Assay

PAF-induced bronchospasm in guinea pigs: Male Hartley guinea pigs (450~550 g) were obtained from Charles River Breeding Laboratories (Wilmington, MA). The animals were fasted overnight and were anesthetized in the morning with 0.9 ml/kg of dialurethane ip (containing 0.1 g/ml of diallylbarbituric acid, 0.4 g/ml of ethylurea and 0.4 g/ml of urethane). The left jugular vein was cannulated for the administration of compounds. The trachea was cannulated and the animals were ventilated by rodent respirator at 55 strokes/minute with a stroke volume of 4 ml. A side arm to the tracheal cannula was connected to a pressure transducer to obtain a continuous measure of inflation pressure. Bronchoconstriction was measured as the percentage of increase in inflation pressure that peaked within 2 minutes after challenge with PAF. The animals were challenged iv with PAF (0.4 μg/kg in isotonic saline containing 0.25% BSA). Each animal was challenged only once. The dose of PAF was selected from preliminary dose-response studies to increase inflation pressure 300~400% (40~50 cm H_2O) or 70 to 80% of the maximum response to PAF. The effect of a compound on the bronchospasm is expressed as percentage of inhibition of the increase in inflation pressure compared to the increase in a corresponding control group.

Results and Discussion

Taxonomy of the Producing Strain

Morphological examination of the producing culture on malt extract agar revealed the formation of unilocular pycnidia, superficial or slightly immersed in the agar. The pycnidia occur singly or in clusters, are subglobose, pale becoming medium brown. Mature pycnidia average 100 μm in height and 125 μm in diameter with a single central ostiole. Conidiophores are absent; the conidia are aseptate, hyaline, thin-walled, $1.5\sim2\times2.5\sim3\,\mu$m, ellipsoid, often biguttulate. Multicellular setae, $20\times3\,\mu$m, may be present near the ostiole.

On malt extract agar colonies grew to 33 mm in diameter and appeared humped in the center and velutinous. Hyaline aerial mycelia were formed along with blackish brown submerged mycelia. Pycnidia were absent from margins but were numerous and large in other regions of the colony.

On malt yeast agar colonies grew to 42 mm in diameter, were low spreading, and velutinous in older regions. Aerial mycelia were hyaline, lanose and in sectors, with blackish brown submerged mycelia in older regions and sectors. Pycnidia were abundant.

Colonies on potato dextrose agar reached 44 mm in diameter, were low and spreading. Colony color was medium brown to dark olive on the surface and dark brown, typically zonate, in reverse. Hyaline aerial mycelia were formed as were abundant pycnidia.

On CZAPEK's Dox agar colonies grew to 47 mm in diameter, were low and spreading. Colony color was drab olive on the surface and darker with marked zonation in reverse. The aerial mycelia were hyaline with brown submeged mycelia. Pycnidia were absent from the colony margin but numerous in other regions of the colony.

Based on morphological and cultural chracteristic the producing culture, SCF-592, was identified as a member of the genus *Phoma*.[11] The culture has been deposited in the American Type Culture Collection, Rockville, Maryland as ATCC 74077.

Fermentation

A typical time course for the fermentation is shown in Fig. 1. The pH decreased from 8 to 4 within 18 hours, accompanied by a similarly rapid drop in the dissolved oxygen concentration. PAF activity was detected at 48 hours and reached its maximum level of activity after 120 hours. At this point the dissolved oxygen concentration was zero and the packed cell volume was at its maximum. The fermentation broth was harvested at this optimal point.

Isolation

The purification of Sch 47918, Sch 49026, Sch 49027 and Sch 49028 was accomplished by EtOAc extraction, gel permeation, precipitation and reverse phase chromatography. The procedure is outlined in Scheme 1. After crystallization from $CHCl_3$ - MeOH (3 : 7), Sch 47918 (20 mg) and Sch 49026 (50 mg) were obtained as white crystals. Sch 49027 (12 mg) and Sch 49028 (11 mg) were obtained as white amorphous powders after lyophilization.

Physico-chemical Properties

Sch 47918, Sch 49027 and Sch 49028 are soluble in chloroform, dichloromethane and dimethyl sulfoxide; partially soluble in ethyl acetate, methanol and acetone; insoluble in water, petroleum ether and hexane. Sch 49026 is soluble in dichloromethane, chloroform and acetone; partially soluble in ethyl acetate,

Fig. 1. Fermentation profile of SCF-592.

○ pH, ■ activity, ▲ PCV, ● dissolved O_2.

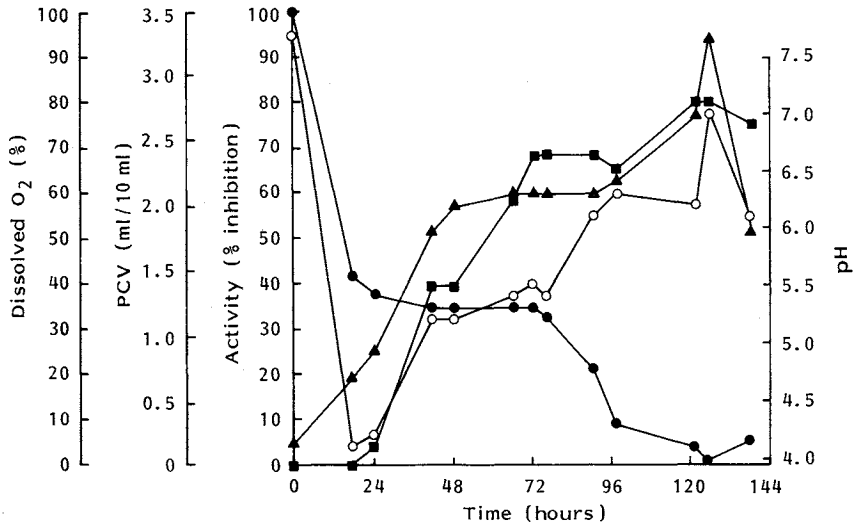

Table 1. Physico-chemical properties of Sch 47918, Sch 49026, Sch 49027 and Sch 49028.

	Sch 47918	Sch 49026	Sch 49027	Sch 49028
MP	204~205°C	73°C	58~60°C	78~80°C
Molecular formula	$C_{20}H_{28}O_3$	$C_{20}H_{32}$	$C_{20}H_{30}O_4$	$C_{20}H_{30}O_4$
CI-MS (*m/z*)	317 $(M+H)^+$	273 $(M+H)^+$	335 $(M+H)^+$	335 $(M+H)^+$
HREI-MS (*m/z*)				
Calcd:	316.2038	272.2504	334.2144	334.2144
Found:	316.2034	272.2499	334.2147	334.2155
$[\alpha]_D^{22}$ ($CHCl_3$)	+222.4° (*c* 0.3)	+110.2° (*c* 0.3)	+74.4° (*c* 0.24)	+245.6° (*c* 0.3)
UV λ_{max}^{MeOH} nm	End, 244 (6,352)	End	End	End
IR (KBr) ν_{max} cm^{-1}	2977, 2887, 1705, 1689, 1625, 1433, 1384, 1198, 896	3013, 2957, 2906, 2843, 1625, 1447, 1383, 901, 861	3433, 2918, 2874, 1632, 1448, 1237, 1058, 884	3431, 2926, 2856, 1623, 1453, 1232, 1053, 962

hexane, methanol and dimethyl sulfoxide; insoluble in water. The compounds were negative in ninhydrin and Rydon tests. The physico-chemical properties of these four components are summarized in Table 1.

Structure Elucidation

The structures of Sch 47918, Sch 49026, Sch 49027 and Sch 49028 were determined based upon spectroscopic data analyses, including MS, UV, IR, ^1H and ^{13}C NMR methods. ^1H and ^{13}C NMR spectra are shown in Tables 2 and 3. Assignments of the protons to the relevant carbons were made by HETCOR experiments, and the quaternary carbons were located by DEPT as well as SINEPT experiments.

As shown in Fig. 2, the proposed structure and stereochemistry of Sch 47918 were established based on extensive spectroscopic studies as well as a single crystal X-ray diffraction analysis. The detail discussion of structure elucidation and X-ray data is published in a separate paper.[12]

The structure of Sch 49026, a relatively non-polar compound was deduced as follows. The molecular weight, 272, was established by CI-MS which showed a protonated molecular ion *m/z* 273 $(M+H)^+$. The molecular formula, $C_{20}H_{32}$ (5 unsaturations), was determined by high resolution EI-MS (*m/z* calcd: 272.2504,

Fig. 2. ORTEP diagram (relative stereochemistry) and solid-state conformation of Sch 47918; small circles represent hydrogen atoms.

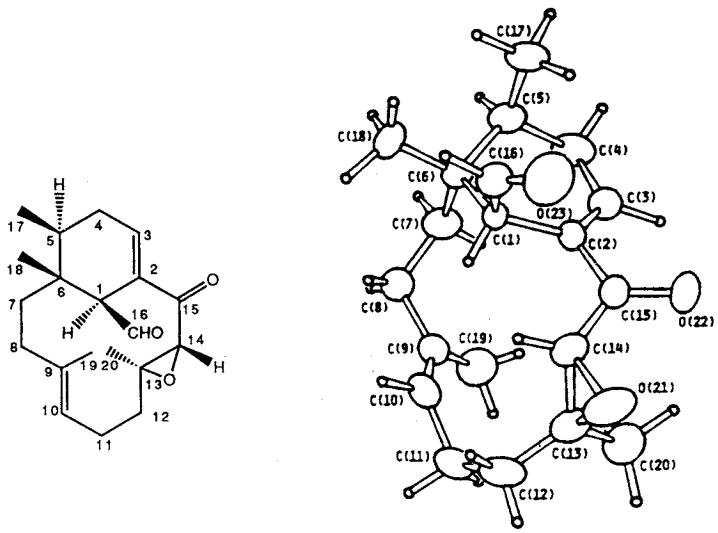

found: 272.2499) and carbon NMR data. UV and IR data (see Table 1) were consistent with the ^{13}C NMR results revealing the absence of oxygenated carbons in the molecule. ^{13}C NMR (DEPT) experiments displayed three trisubstituted double bonds as well as the presence of six methylene, two methine and five methyl groups. The ^{1}H NMR spectrum showed three olefinic protons at 4.95, 5.11, 5.28 ppm indicating three trisubstituted double bonds. Five methyl groups showing two doublets and three singlets at 0.84, 1.11, 0.91, 1.50 and 1.55 ppm were assigned to connected with two methines (C-1, C-5), a quarternary carbon (C-6) and two unsaturated carbons (C-9, C-13), respectively, based upon COSY, HETCOR and SINEPT spectral data. The ^{1}H and ^{13}C NMR assignments are listed in Tables 2 and 3. All evidence strongly suggested that Sch 49026 possessed the same carbon skeleton as Sch 47918 in comparison with their spectra. Thus, the structure of Sch 49026 is proposed, as shown in Fig. 3. The stereochemistry is assumed to be the same as Sch 47918 because Sch 49026 is a putative biosynthetic precursor of Sch 47918.

Two additional analogues, Sch 49027 and Sch 49028, were both found to have the same molecular weight 334 on the basis of CI mass spectrometric data that showed a protonated molecular ion *m/z* 335 $(M+H)^+$. The molecular formula was established as $C_{20}H_{30}O_4$ for both compounds based on high resolution EI-MS (*m/z* calcd: 334.2144, found: 334.2147; calcd: 334.2144, found: 334.2155, respectively) and carbon NMR data. Similar UV (end absorption) and IR (3430 cm^{-1}, broad, OH) were observed for these two molecules. Although similarities were found in these two compounds, their spectral data were further scrutinized to determine the differences in their structures.

The ^{1}H and ^{13}C NMR data of Sch 49028, including COSY, DEPT, HETCOR and SINEPT experiments, indicated an olefinic proton signal at 5.42 ppm coupling with an unsaturated carbon at 130.4 (d) ppm. This unsaturated carbon (C-10) together with another three vinylic carbons reflected one trisubstituted and one tetrasubstituted double bond. A distinctive dioxy-quaternary carbon (C-15) at 108.4 (s) ppm clearly revealed the presence of a ketal or hemiketal group. An AB quartet proton signal at 4.61 ppm correlating with an oxygenated carbon at 71.55 (t) ppm the in HETCOR spectrum suggested the

Table 2. ^{1}H NMR chemical shift assignments and coupling data of Sch 47918, Sch 49026, Sch 49027 and Sch 49028[a].

Proton	Sch 47918	Sch 49026	Sch 49027	Sch 49028
1-CH	3.80 br s	1.07~1.18 m	4.16~4.24 m	—
3-CH	6.96 br s	5.28 d (J=3.0 Hz)	3.19 OH[b]	4.08~4.17 m
4-CH_2	1.86~2.68 m	1.90~2.45 m	1.42~1.93 m	1.61~1.72 m
5-CH	1.50~1.65 m	1.55~1.68 m	2.10~2.22 m	2.67~2.82 m
7-CH_2	1.75 dd (J=7.8, 14.3 Hz)	1.45~2.08 m	1.58~2.41 m	1.68~2.35 m
8-CH_2	1.88~2.35 m	2.07~2.27 m	1.70~1.98 m	1.92~2.49 m
10-CH	5.23 br d (J=12.1 Hz)	4.95 br t (J=6.5 Hz)	4.90 br d (J=8.7 Hz)	5.42 br d (J=11.7 Hz)
11-CH_2	1.90~2.44 m	1.90~2.28 m	1.53~2.42 m	1.32~2.45 m
12-CH_2	1.12~2.10 m	1.20~1.90 m	1.55~2.00 m	1.15~1.81 m
14-CH	3.47 s	5.11 t (J=7.2 Hz)	2.92 s	3.62 br s
15	—	2.60~2.85 m (CH_2)	4.16 OH[b]	4.19 OH[b]
16	9.90 d (J=1.2 Hz, CHO)	0.84 d (J=7.1 Hz)	4.30 dd (J=3.0, 13.2 Hz), 4.50 dd (J=1.6, 13.2 Hz)	4.47, 4.72 AB q (J=12.9 Hz)
17-CH_3	0.88 d (J=7.1 Hz)	1.11 d (J=7.0 Hz)	0.91 d (J=7.1 Hz)	0.91 d (J=7.2 Hz)
18-CH_3	1.32 s	0.91 s	1.51 s	1.23 s
19-CH_3	1.60 s	1.55 s	1.64 s	1.63 s
20-CH_3	1.11 s	1.50 s	0.99 s	0.89 s

[a] Measured at 300 MHz in $CDCl_3$; chemical shifts in ppm from TMS.
[b] Exchangeable with D_2O, and assignments are interchangeable.

Table 3. ^{13}C NMR chemical shift assignments of Sch 47918, Sch 49026, Sch 49027 and Sch 49028[a,b].

Carbon	Sch 47918	Sch 49026	Sch 49027	Sch 49028	Carbon	Sch 47918	Sch 49026	Sch 49027	Sch 49028
1	53.00 d	40.85 d	63.83 d	127.2 s	11	35.02 t	33.04 t	34.97 t	36.49 t
2	133.3 s	134.2 s	131.9 s	144.0 s	12	38.06 t	33.55 t	38.35 t	37.32 t
3	137.9 d	121.3 d	148.1 s	61.03 d	13	63.26 s	139.1 s	60.49 s	79.16 s
4	30.95 t	30.94 t	32.47 t	32.95 t	14	64.18 d	127.3 d	66.45 d	73.97 d
5	35.95 d	37.12 d	30.89 d	26.52 d	15	203.0 s	34.60 t	108.1 s	108.4 s
6	40.15 s	38.23 s	38.35 s	36.90 s	16	193.7 d	17.08 q	69.48 t	71.55 t
7	34.35 t	39.51 t	34.19 t	33.55 t	17	17.43 q	13.25 q	16.85 q	16.33 q
8	24.69 t	24.22 t	23.66 t	24.90 t	18	21.80 q	21.67 q	21.42 q	21.58 q
9	137.9 s	136.5 s	134.4 s	129.1 s	19	16.00 q	16.56 q	20.94 q	18.90 q
10	125.0 d	122.6 d	128.5 d	130.4 d	20	14.41 q	14.98 q	14.38 q	14.51 q

[a] Measured at 75 MHz in $CDCl_3$, chemical shifts in ppm from TMS.
[b] Multiplicity was determined by DEPT data.

Fig. 3. Structure of Sch 49026.

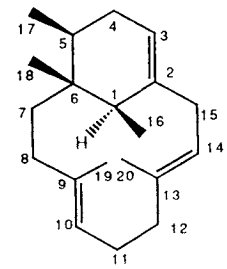

presence of an allylic oxygenated methylene group at position-16. The HETCOR spectral data also showed a singlet proton signal at 3.62 ppm correlating with an oxygenated carbon at 73.97(d) ppm. This carbon (C-14) together with another quaternary carbon at 79.16(s) ppm were assigned to a trisubstituted epoxide. A broad singlet proton signal at 4.11 ppm attached to a carbon at 61.03(d) ppm indicating a secondary allylic hydroxyl group at position-3. The arrangement of the rest of methylene and methyl groups was expected to the similar to Sch 47918. As shown in Fig. 4, SINEPT experiments suggested the hemi-ketal group in the position between the epoxide and the tetrasubstituted double bond, and the secondary hydroxyl group adjacent

Fig. 4. Stereoscopic drawing and structure of Sch 49028 as revealed by SINEPT experiments.
Arrows indicate ^{1}H-^{13}C long range couplings.

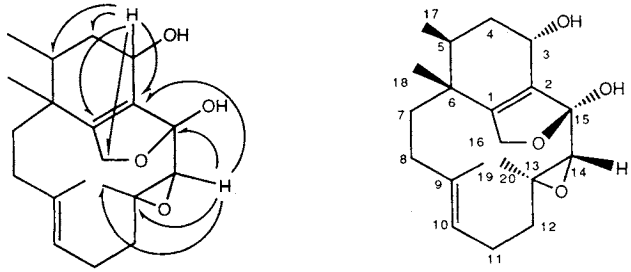

Fig. 5. Structure of Sch 49027.

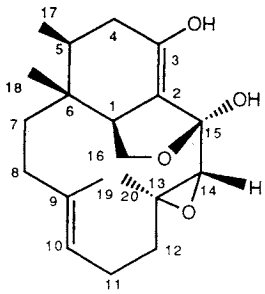

Table 4. Inhibition of *in vitro* PAF-induced platelet aggregation by Sch 47918, Sch 49026, Sch 49027 and Sch 49028.

PAF activity	Sch 47918	Sch 49026	Sch 49027	Sch 49028
IC_{50} (μM)	6.96	>36	1.68	1.26

to this double bond. The assignment of a five membered ring linked through the ketal-oxygen to methylene carbon was also supported by SINEPT data. The stereochemistry of Sch 49028 was proposed as shown in Fig. 4 based on a direct correlation with Sch 47918 which was determined by X-ray analysis. However, the chiral center at carbon-3 could not be correlated with Sch 47918. The stereochemistry at carbon-3 was determined by NOE experiment. The absence of an NOE signal of proton-5 by irradiation of proton-3 suggested that these two protons are *trans*-oriented. (see Fig. 4).

Sch 49027 was found to be a closely related isomer of Sch 49028 with the double bond shifted from the 1,2-position to the 2,3-position on the basis of spectral data analysis. The key evidence in the carbon NMR data indicated that the carbon-3 signal was shifted to a typical oxygen-attached olefinic range at 148.1(s) ppm, while the methine carbon (C-1) moved to 63.83(d) ppm because of the double bond shift. The chemical shift of the AB quartet which was assigned to methylene protons moved slightly up-field to 4.40 ppm, and was further coupled to the adjacent methine proton at 4.18 ppm. All assignments for the remaining part of the molecule were comparable to Sch 49028. Both ^{1}H and ^{13}C NMR spectra data strongly suggested the presence of an enol functionality in the molecule. Based on these data, the structure of Sch 49027 is proposed and shown in Fig. 5.

Biological Properties

The broth filtrate from this culture was initially identified as active in a PAF receptor binding assay using rabbit platelets and [^{3}H]-PAF essentially as described by HWANG *et al.*[13] Subsequently, identification and characterization of the active fractions was assessed using inhibition of PAF-induced human platelet aggregation. Table 4 shows the IC_{50} values for inhibition of PAF-induced platelet aggregation *in vitro* using freshly prepared human platelet rich plasma. Sch 49028 was the most potent inhibitor having an IC_{50} value of 1.26 μM. Sch 49026 showed poor solubility in the assay system.

Further evidence that Sch 49028 antagonizes [^{3}H]-PAF binding is that its inhibitory potency decreases

with increasing PAF concentration. The IC_{50} values for Sch 49028 are 1.2 μM at 10 nM PAF, 3.0 μM at 25 nM PAF and 11.1 μM at 50 nM PAF. This result would not be expected if this compound were acting in a non-specific manner to block platelet aggregation. Taken together, these results indicate that Sch 49028 acts by competition with PAF for receptor binding.

The most potent compound, Sch 49028 was further tested for *in vivo* anti-PAF activity, measured as inhibition of PAF-induced bronchospasm in guinea pigs. This compound was found to be inactive (0% inhibition, $n=2$) at 5 mg/kg, iv. All these compounds were not active against and Gram-positive, and Gram-negative bacteria as well as fungi (*Candida* sp.) in agar diffusion assays (>30 μg/disc).

Conclusion

Novel PAF antagonists, Sch 47918, Sch 49026, Sch 49027 and Sch 49028, have been isolated from a *Phoma* sp. A bicyclic diterpene, verticillol,[14] a plant natural product isolated from the wood of *Sciadopitys verticillata* Sieb. et Zucc (Taxodiaceae) has a similar macrocyclic ring system. However, it should be noted that the carbon skeleton of the PAF inhibitors described above is different from verticillol because of a rearrangement of the methyl group from carbon-1 to carbon-6 in the molecules. A structurally related compound, phomactin B, was recently reported as a PAF inhibitor.[15] These PAF antagonists are new members of the rare cleomane class of diterpenes, the only previous example being cleomeolide.[16,17]

Acknowledgments

We thank Dr. P. DAS, Mr. R. MALCHOW and Mr. P. BARTNER for CI, FAB-MS and HREI-MS data, Mrs. J. PETRIN for *in vitro* PAF-assay data. We also thank Professor T. NORIN for suppling a sample of verticillol.

References

1) HENSON, P. M. & R. N. PINCKARD: Basophil-derived platelet-activating factor (PAF) as an *in vivo* mediator of acute allergic reactions: Demonstration of specific desensitization of platelets to PAF during IgE-induced anaphylaxis in the rabbit. J. Immunol. 119: 2179~2184, 1977
2) KNAUER, K. A.; L. M. LICHTENSTEIN, N. F. ADKINSON, Jr. & J. E. FISH: Platelet activation during antigen-induced airway reactions in asthmatic subjects. N. Engl. J. Med. 304: 1404~1407, 1981
3) WEISS, H. J.: Platelet physiology and abnormalities of platelet function. N. Engl. J. Med. 293: 580~588, 1975
4) PRESCOTT, S. M.; G. A. ZIMMERMAN & T. M. MCINTYRE: Platelet activating factor. J. Biol. Chem. 265: 17381~17384, 1990
5) OKAMOTO, M.; K. YOSHIDA, M. NISHIKAWA, T. ANDO, M. IWAMI, M. KOHSAKA & H. AOKI: FR-900452, a specific antagonist of platelet activating factor (PAF) produced by *Streptomyces phaeofaciens*. I. Taxonomy, fermentation, isolation, and physico-chemical and biological characteristics. J. Antibiotics 39: 198~204, 1986
6) OKAMOTO, M.; K. YOSHIDA, M. NISHIKAWA, M. KOHSAKA & H. AOKI: Platelet activating factor (PAF) involvement in endotoxin-induced thrombocytopenia in rabbits: studies with FR-900452, a specific inhibitor of PAF. Thromb. Res. 42: 661~671, 1986
7) OKAMOTO, M.; K. YOSHIDA, I. UCHIDA, M. KOHSAKA & H. AOKI: Studies of platelet activating factor (PAF) antagonists from microbial products. II. Pharmacological studies of FR-49175 in animal models. Chem. Pharm. Bull. 34: 345~348, 1986
8) OKAMOTO, M.; K. YOSHIDA, I. UCHIDA, M. NISHIKAWA, M. KOHSAKA & H. AOKI: Studies of platelet activating factor (PAF) antagonists from microbial products. I. Bisdethiobis (methylthio)gliotoxin and its derivatives. Chem. Pharm. Bull. 34: 340~344, 1986
9) YOSHIDA, K.; M. OKAMOTO, N. SHIMAZAKI & K. HEMMI: PAF inhibitors of microbial origin, studies on diketopiperazine derivatives. Prog. Biochem. Pharm. 22: 66~80, 1988
10) JONG, S. C. & M. J. EDWARDS, (*Eds.*): The American Type Culture Collection Cataloque of Filamentous Fungi. 18th Edition. American Type Culture Collection, Reckville, Maryland, 1991
11) BOEREMA, G. H. & G. J. BOLLEN: Conidiogenesis and conidial septation as differentiating criteria between *Phoma* and *Ascochyta*. Persoonia 8: 111~114, 1975
12) CHU, M.; M. G. PATEL, V. G. GULLO, I. TRUMEES, M. S. PUAR & A. T. MCPHAIL: Sch 47918, a novel PAF

antagonist from the fungus *Phoma* sp. J. Org. Chem. 57: 5817~5818, 1992

13) HWANG, S.-B.; C. S. C. LEE, M. J. CHEAH & T. Y. SHEN: Specific receptor sites for 1-*O*-alkyl-2-*O*-acetyl-*sn*-glycero-3-phosphocholine (platelet activating factor) on rabbit platelet and guinea pig smooth muscle membranes. Biochemistry 22: 4756~4763, 1983

14) KARLSSON, B.; A.-M. PILOTTI, A.-C. SÖDERHOLM, T. NORIN, S. SUNDIN & M. SUMIMOTO: The structure and absolute configuration of verticillol, a macrocyclic diterpene alcohol from the wood of *Sciadipitys verticillata* Sieb. et Zucc. (Taxodiaceae). Tetrahedron 34: 2349~2354, 1978

15) SATO, A.; M. SUGANO, T. OSHIMA, H. HARUYAMA & K. FURUYA (Sankyo): Jpn. Pat. 03,216,197 ('91) [91,216,197], Sept. 24, 1991

16) MAHATO, S. B.; B. C. PAL, T. KAWASAKI, K. MIYAHARA, O. TANAKA & K. YAMASAKI: Structure of cleomeolide, a novel diterpene lactone from *Cleome icosandra* Linn. J. Am. Chem. Soc. 101: 4720~4723, 1979

17) BURKE, B. A.; W. R. CHAN, V. A. HONKAN, J. F. BLOUNT & P. S. MANCHAND: The structure of cleomeolide, an unusual bicyclic diterpene from *Cleome viscosa* L. (Capparaceae). Tetrahedron 36: 3489~3493, 1980